Inter-Vehicle Cooperation Channel Estimation for IEEE 802.11p V2I Communications

Yan Yang, Dan Fei, and Shuping Dang

Abstract: **The impact of imperfect channel state information (CSI) is particularly serious in vehicle-to-infrastructure (V2I) and vehicle-to-vehicle (V2V) communications. Considering the sparse characteristics of V2I channels, this paper proposes an inter-vehicle cooperation channel estimation (IVC-CE) method at the IEEE 802.11p physical layer, and the effects of outdated CSI can be mitigated by single or multiple vehicle measurements. With these assisted measurements, we can develop an interpolation-assisted channel estimation technique to obtain accurate CSI. To select optimum measurements from a group of channel estimates, we utilize the position and velocity of a vehicle as a priori information. We investigate the validity of the IVC-CE technique with the traditional linear minimum mean-squared error algorithm and present a scalable data transmission scheme at the physical layer. The performance of IVC-CE is analyzed by its mean squared error and bit error rate in a fast fading channel environment. Simulations and numerical results show the merits of the proposed techniques, which can significantly enhance estimation performance and support safety related data transmissions for vehicular ad hoc networks.**

Index Terms: **Channel state information (CSI), channel estimation (CE), IEEE 802.11p, interpolation, inter-vehicle cooperation (IVC).**

I. INTRODUCTION

IEEE 802.11p has been standardized with great expectations to provide safety, navigation, and automation applications in modern intelligent transportation systems (ITS). The physical layer of IEEE 802.11p is based on the widely used IEEE 802.11a standard, a matured orthogonal frequency division multiplexing (OFDM) technology that mainly focuses on nomadic indoor usage [1]. IEEE 802.11p would play a key role in dedicated short-range communication (DSRC) and wireless access for vehicular environments (WAVE). In a typical emergency scenario, e.g., a car collision in a highway, the warning message should be timely diffused to the car drivers via a typical safety related application. In recent years, vehicle-to-infrastructure (V2I) communications for safety has been proposed, and is expected to enable the wireless exchange of safety related data between vehicles and roadway infrastructure, so as to avoid motor vehicle crashes. According to preliminary studies of U.S. Department of Transportation, V2I wireless technology will be employed to reduce, mitigate, or prevent an additional 12% of crash scenarios which is not addressed by the vehicle-to-vehicle (V2V) program [2]. In IEEE 802.11p standard, 8 different coding and modulation schemes are defined to achieve different data rates, and the knowledge of timely channel state information (CSI) at the transmitter needs to be known for power control, scheduling, and data demodulation. However, timely CSI is difficult to obtain in fast time-varying fading environment, and the outdated CSI has a severe impact on the system performance [3]. This situation would be particularly serious in V2I communication scenarios, owing to a wide range Doppler shift and rapidly time-varying channels.

OFDM channel estimation has been extensively studied [4]–[10]. In general, channel estimation can be classified as blind and non-blind estimation, where the blind estimation uses no training or pilot symbols and non-blind estimation uses a data-aided (DA) or pilot-aided (PA) approach. Several familiar criteria, such as minimum mean square error (MMSE), maximum likelihood (ML) and least square (LS) methods have been well investigated to estimate CSI at a certain time-frequency grid specified by the pilot symbols [11]. However, a considerable amount of research is for quasi-static channel estimation. Recently, the fast time-varying channel estimation has received more attention [12]–[14]. The difficulties of fast time-varying channel estimation mainly come from two aspects: 1) Channel estimation errors are influenced by multiple factors, including noise, interference and channel time variations 2) outdated CSI is caused by both of the feedback delay and computational complexity. Pilot-symbol-aided parameter estimation and effects of channel statistics (e.g., Doppler shift) have been well studied. Ye *et al.* [12] examined the effects of channel estimation error and outdated CSI, and proposed the use of multiple estimates to tolerate larger errors or a longer delay in CSI. Şenol *et al.* [13] proposed a non-data aided joint channel estimation method, and discussed an interpolation and prediction technique to mitigate the effects of imperfect or impartial CSI. Manolakis *et al.* [15] studied a time domain channel prediction method based on a Doppler-delay model of the time-variant radio channel, and cooperative base stations with larger feedback delays and higher mobility were considered. Moreover, [16] showed that limited CSI feedback could have a flexible transmission delay in wireless communications. Compressed sensing has also been used to the channel estimation because of the sparsity of the outdoor channels [17]. In practice, IEEE 802.11p is derived from IEEE 802.11a that was designed for low mobility or relatively sta-

Manuscript received October 27, 2016.

This work was in part supported by the research task of the State Key Laboratory of Rail Traffic Control and Safety (RCS2017ZT010), the China Scholarship Council, and the key research task of the Ministry of Education of the People's Republic of China (Grant No. K13C800010). This paper was presented in part at IEEE VTC2016-Spring, Nanjing, China, May 2016.

Yan Yang and Dan Fei are with the State Key Laboratory of Rail Traffic Control and Safety, Beijing Jiaotong University, Beijing, 100044 China, email: yyang@bjtu.edu.cn, dfei@bjtu.edu.cn.

Shuping Dang is currently a D.Phil candidate with the Department of Engineering Science, University of Oxford, email: shuping.dang@eng.ox.ac.uk.

Y. Yang is the corresponding author.

Digital object identifier: 10.1109/JCN.2017.000040

tionary indoor environments, thus, V2I/V2V channel estimation may be greatly challenging due to the motion-based Doppler spread and inherent channel nonstationarities [18]–[22].

The issue on which we concentrate in this paper is how to mitigate the impacts of imperfect CSI in V2I communications. We devote to developing an estimation technique based on inter-vehicle cooperative measurements. We mainly consider two key issues about V2I channel estimation: 1) How to obtain timely CSI in V2I communications, assisted by foreknown position or velocity information of cooperative vehicle. 2) How to determinate the cooperative vehicle and thereby improve the performance of V2I communications. The main contributions of this paper are summarized as follows:

- We propose a new IVC-CE methodology for V2I communications and use multiple cooperative measurements to mitigate the impacts of imperfect CSI. By using linear MMSE (LMMSE) method based on singular value decomposition (SVD), we investigate a pilot-aided channel estimation method, so that it can be utilized in different mobility scenarios, e.g., urban, suburban and highway. In particular, we derive an approach of IVC-CE that can apply multiple measurements to obtain accurate CSI and mitigate the impacts of outdated CSI.
- In our proposed scheme, the position and velocity of the vehicle can be exploited as a priori information, which is helpful to select optimum measurements from a group of channel estimates. Based on this idea, we subsequently develop a simplified mechanism, which can effectively select the appropriate cooperative vehicles in the highway scenario to estimate the real-time channel parameters.
- We investigate the solution of the safety related data transmission, which might be one of the most important applications for safety communication in vehicular ad hoc networks (VANETs). We further develop a scalable data transmission method at the physical layer, which is capable of reducing bit error rate (BER) and supporting safety related data transmissions, e.g., real-time and reliable message dissemination.

The remainder of this paper is organized as follows: In Sections II and III, we separately describe the IVC-CE model and formulate the mechanism for user cooperation. In Section IV, we propose the fundamentals of the linear interpolation estimator, and introduce the channel estimation algorithm based on the single/multi-user collaboration. Simulations and numerical results are described in Section V, and we conclude the paper in Section VI.

II. SYSTEM MODEL

Considering a V2I communication channel from a roadside infrastructure or access point (AP) to a mobile station (MS) receiver without any relay, there exist only one transmit antenna and one receive antenna at the AP and each vehicle receiver, respectively. Within a certain distance range, we assume there are at least two vehicles driving in the same direction and their data transmission occurs in different time slots on the same carrier frequency. Fig. 1 illustrates the proposed IVC-CE model, where $h(x, y; \tau; t)$ represents the channel impulse response (CIR) at the determined position (x, y) and $t = t_1, t_2, \cdots, t_n$ denoting different time slots. To describe the main concepts, the following parameters are defined.

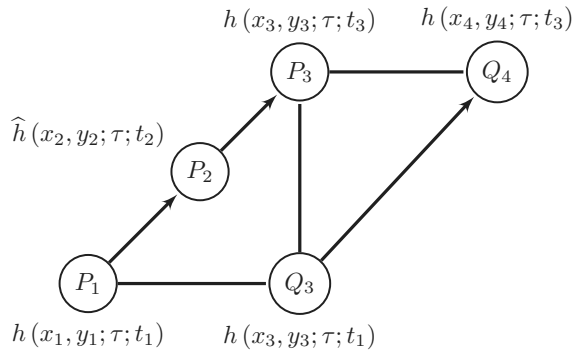

Fig. 1. Inter-vehicle cooperative channel estimation model.

Table 1. Summary of notations and symbols.

Notation	Representation of the symbol
P	Master vehicle
Q	Cooperative vehicle
u	Position index of P, $u = 1, 2, \cdots$
v	Position index of Q, $v = 1, 2, \cdots$
P_u^i	Position set (x_u, y_u) of ith P, or P_u $(i = 1)$
Q_v^j	Position set (x_v^j, y_v^j) of jth Q, or Q_v $(j = 1)$
τ	Input delay of the channel
h_u^i	$h\left(x_u^i, y_u^i; \tau; t\right)$ of ith P at (x_u, y_u)
h_v^j	Historitic $h\left(x_v^j, y_v^j; \tau; t\right)$ of jth Q at (x_v, y_v)
$\widehat{h}_{u+1}$	Upcoming $h(x_{u+1}, y_{u+1}; \tau; t)$ of P

As shown in Fig. 1, the master vehicle P moves from P_1 to P_3, and a cooperative vehicle Q moves from Q_3 to Q_4 simultaneously. It is clear that when P and Q are moving at a high speed, all of the CIR estimates become outdated. Correspondingly, when P and Q pass through the same position, we can obtain two sets of highly similar CIRs denoted by h_u and h_v at different measurement times. In this paper, we further propose using a set of spatial related estimates to mitigate the effect of CSI errors. Especially, we extend the approach proposed in [12], which used multiple estimates from different frequencies or times to tolerate larger errors in channel estimation or longer delay in CSI.

Considering a typical line of sight (LOS) V2I channel in highway environments, the scattering is sparse, resulting in a highly correlated channel. We suppose estimated $\widehat{h}_{u+1}$ are measured at a fixed scattering area, i.e., the number of the scatterers and their positions are fixed[1]. By observing $h(x_3, y_3; \tau; t_3)$ at P_3 and $h(x_3, y_3; \tau; t_1)$ at Q_3, we can see that these two CIRs are associated with the same position, and the power delay profiles (PDPs) are similar. At this fixed position, the radio channels can be viewed as time-invariant, and these two observations at different times would be found to be highly similar. Hence, it is reasonable to suppose that the current estimated parameters of $\widehat{h}(x_2, y_2; \tau; t_2)$ might be more accurate by using historical obser-

[1]Around the position P_{u+1} (e.g., radius $\Upsilon \leq 3$ m in highway), we suppose the scattering under the macrocell environment is identical. At this same position, the CIR observation of Q occurred 3.6 s before if the distance $\|P - Q\| = 100$ m and $v = 90$ km/h (25 m/s). Assuming the distance constraint of Υ is small enough, e.g., $\Upsilon < 0.5$ m, it is applicable for a more complex urban environment.

vations from the positions of P_1 and Q_3.

Based on this model, we consider an OFDM system where the grouped transmission symbols are modulated by the inverse discrete Fourier transform (IDFT) on to N parallel subcarriers. Then, the aggregate OFDM symbol $\tilde{S}(t)$, without cyclic prefix, can be written as

$$\tilde{S}(t) = \sum_{k=0}^{N-1} S_k e^{j2\pi kt/T}, \qquad 0 \le t < T, \tag{1}$$

where S_k is the transmission data, N is the number of subcarriers and T is the symbol duration.

To simplify the analysis, we consider the vehicle moving on a 2-D plane with respect to AP, where AP is at the coordinate origin[2]. As a result, we can directly obtain the distances among different vehicles, e.g., $\|P_u\|$: the distance between AP and Q, $\|Q_v\|$: the distance between AP and cooperative vehicle, and $\|P_u - Q_v\|$: the distance between P and Q. For the master receiver at the uth position, denoting $\tilde{S}_{n,u}(t)$ as signal transmitted over the nth path, we can write the received signal without noise in the form as

$$r_u(t) = \mathrm{Re}\left\{\sum_{n=1}^{L} C_{n,u} e^{j\varphi_{n,u}(t)} \tilde{S}_{n,u}(t - \tau_{n,u})\right\}, \tag{2a}$$

$$\varphi_{n,u}(t) = \varphi_{n,u} - 2\pi c\tau_{n,u}/\lambda_c + 2\pi f_{D_u,n} t, \tag{2b}$$

where $C_{n,u}$, $\varphi_{n,u}(t)$, $f_{D_u,n}$, $\tau_{n,u}$ are the propagation gain, phase, maximum Doppler shift and propagation path delay varying in the position index u, which are associated with the nth propagation path; L is the total number of paths; λ_c is the wavelength of carrier and c is the speed of light [23].

One can see that $\tau_{n,u}$ is determined by the total travelling distance D_n of the nth plane wave, i.e., $D_n = D_n^{A-S} + D_n^{S-V}$. Here, D_n^{A-S} is the distance between AP and the scatterer, and D_n^{S-V} is the distance between the scatterer and the position of vehicle's observation. Similarly, the maximum Doppler shift $f_{D_u,n}$ is dominated by the local *angle-of-arrival* (AOA) α_n^R and the local *angle-of-motion* (AOM) α_ϑ^R, by the relation $f_{D_u,n} = f_{\max}\cos\left(\alpha_n^R - \alpha_\vartheta^R\right)$. α_n^R and α_ϑ^R are also determined by the wave travelling distance [24], [25]. Mathematically, the CIR is derived by [12], i.e.,

$$h_u(t,\tau) = \sum_{n=1}^{L} C_{n,u} e^{j\varphi_{n,u}(t)} \delta(\tau - \tau_{n,u}(t)). \tag{3}$$

Because the outdoor wireless channels exhibit sparse structure, without loss of generality, we can set the maximum multipath components $L = 4$ in a typical highway environment.

As shown in Fig. 1, the movement of a vehicle is regular on the road, and the motion trajectory would be highly similar on the highway. For example, vehicle P and Q pass through a same position $h(x_3, y_3; t, \tau)$ at time t_3 and t_1, respectively. At the same position in which different vehicles pass through, the AOA might be highly similar, and we thus devote to designing a method by which the position related channel estimation can be exploited to improve the channel estimation performance. By this way, $h_u(t,\tau)$ is equivalent to $h(x, y; \tau)$, which indicates that variation is related to the vehicle's position, so that the CIR can be modeled as a stochastic process that varies with the position and given by

$$h_u(x, y; \tau) = \sum_{n=1}^{L} C_{n,u} e^{j\varphi_{n,u}(x,y)} \delta(\tau - \tau_{n,u}(x, y)). \tag{4}$$

Referring to Fig. 1, we define h_u^n as the nth observation of P, and let

$$\begin{array}{ll} \mathbf{h}_u^n : \{h_u^1 \cdots h_u^n\} & [x_i, y_i : x_j, y_j] \quad \forall P \\ \mathbf{h}_v^n : \{h_v^1 \cdots h_v^n\} & [x_i, y_i : x_j, y_j] \quad \forall Q \end{array} \tag{5}$$

be the independent observation sets. We suppose that estimated P_{u+1} is located at a fixed scattering area, i.e., the number of the scatterers and their positions are fixed. Let $\mathbf{h}_u$ and $\mathbf{h}_v$ be the stochastic measurement events with respect to the identical position $(\bar{x}, \bar{y}) : \{(\bar{x}_1, \bar{y}_1) \cdots (\bar{x}_n, \bar{y}_n)\} \in [x_i, y_i : x_j, y_j]$. All observations of $\mathbf{h}_u$ and $\mathbf{h}_v$ are generated at the constant vehicle speed, where v_P^i and v_Q^j are the speed of the ith P and the jth Q, respectively, and we further assume $v_P^i = v_Q^j$. As a result, when $n \to \infty$, $\mathbf{h}_u$ converges to $\mathbf{h}_v$. Now, it is intuitive that the value of $h(x_3, y_3; \tau; t_3)$ could be extracted from $h(x_2, y_2; \tau; t_1)$ as a priori observed value. Therefore we have

$$\lim_{|t_3 - t_1| \to 0, v_P^1 = v_Q^1} \underbrace{h(x_3, y_3; \tau; t_3)}_{P_3} = \underbrace{h(x_3, y_3; \tau; t_1)}_{Q_3}, \tag{6}$$

where t_3 is the current time, and t_1 is the historical time. Eq. (6) implies that the positions of historical observations should be the closest. For the historical observation $\mathbf{h}_n^j$, the optimal estimation of upcoming h_{u+1} can be obtained by a subset from $\mathbf{h}_n^j$, which corresponds to the closest element to the position P_{u+1}. The estimated $\widehat{h}(x_{u+1}, y_{u+1}; \tau)$ of interest can be better fitted by a set of spatial related observations $\mathbf{h}_u$, $\mathbf{h}_v^n$, $n = 1, 2, \cdots, N$, which are the closest to the position P_{u+1}. We define Υ as the closest distance between the upcoming position (x_{u+1}, y_{u+1}) and the historical observation position (x_v, y_v). Thus, the optimal $\widehat{h}(x_{u+1}, y_{u+1}; \tau)$ can be calculated by

$$P_{u+1} : \hat{h}_{u+1}(n,k) = \mathbf{\Phi}\left[h_u(n,k), h_v^1(n,k), h_v^2(n,k), \cdots\right]\Big|_{\Upsilon=0}. \tag{7}$$

Without loss of generality, $\mathbf{\Phi}$ can be regarded as a function, such as interpolation, polynomial fitting and so on [26], [27]. Since the same or adjacent lanes in one position might also belong to the same scattering environment, (7) can be extended to a multi-user cooperation scenario. By historical observations P_u, $\mathbf{h}_v^i : \left\{h_v^1, h_v^2, \cdots, h_v^i\right\}$ and Q_v^i, the upcoming estimate h_{u+1} can be estimated by the following two steps.

First step: Let $\widehat{\mathbf{h}}_u^n$, $\widehat{\mathbf{h}}_v^n$ be the estimated CIRs of P and Q obtained by performing n times channel estimates between position index (x_i, y_i) and (x_j, y_j), and each measurement is at the identical position index $(\bar{x}_n, \bar{y}_n), n = 1, 2, \cdots, N$. Let $\mathbf{h}^n$ be the real CIR. According to (5), $\widehat{\mathbf{h}}_u^n$, and $\widehat{\mathbf{h}}_v^n$ have the same propagation plane. Furthermore, applying the law of large numbers (LLN), if $v_P^i = v_Q^j$, $\widehat{\mathbf{h}}_u^n$, $\widehat{\mathbf{h}}_v^n$ converge in probability to

[2]Note that, this model can also be easily extended to 3-D Euclidean space if required.

$\mathbf{h}^n$ [28]. Therefore, for all observations $\widehat{h}_u^n$, $\widehat{h}_v^n$ has the properties:

$$\mathbf{Pr}\left\{\lim_{n\to\infty}\widehat{\mathbf{h}}_u^n=\widehat{\mathbf{h}}_v{}^n\right\}=1 \quad \text{and} \quad \lim_{n\to\infty}\mathrm{E}\left[\left|\mathbf{h}_u^n-\widehat{\mathbf{h}}_v^n\right|^2\right]=0. \quad (8)$$

Clearly, as long as the conditions given in (8) can be satisfied by $\widehat{\mathbf{h}}_v^n$, $\widehat{\mathbf{h}}_u^n$ will converge to $\widehat{\mathbf{h}}_v^n$. Meanwhile, with a sufficiently large generated number of observations within $[x_i, y_i : x_j, y_j]$, (8) is still valid.

According to (3), we can denote $g_{n,u}(t) = C_{n,u}e^{j\varphi_{n,u}(t)}$ as the complex envelope and the CIR at the nth tone of the kth OFDM block can thus be expressed by

$$h_u(n,k)=\sum_{i=0}^{L-1} g_{i,u}(n,k)\delta_{i,u}(n,k)e^{-j2\pi k\Delta f\tau_{i,u}}+n_u(n,k)\ \ \forall\, P_u \quad (9)$$

and

$$h_v(n,k)=\sum_{i=0}^{L-1} g_{i,v}(n,k)\delta_{i,v}(n,k)e^{-j2\pi k\Delta f\tau_{i,v}}+n_u(n,k)\ \ \forall\, Q_v. \quad (10)$$

According to the statistical properties of the non-isotropic scattering studied in [19] and [29], let $g_{u,k}$ be the kth fading envelope of P and the autocorrelation functions of multiple fading envelopes as well as the squared envelope autocorrelation functions of P_u and $\left\{Q_v^1, Q_v^2, \cdots, Q_v^m\right\}$, are given by

$$\begin{cases}\phi_{g_{k,u}g_{k,u}}(\tau_u)=\dfrac{I_0\left(\sqrt{\mathcal{K}^2-4\pi^2 f_{D_u}^2\tau_u^2+j4\pi\mathcal{K}\cos\theta_p f_{D_u}\tau_u}\right)}{I_0(\mathcal{K})}\\ \phi_{g_{k,v}g_{k,v}}(\tau_v)=\dfrac{I_0\left(\sqrt{\mathcal{K}^2-4\pi^2 f_{D_v}^2\tau_v^2+j4\pi\mathcal{K}\cos\theta_p f_{D_v}\tau_v}\right)}{I_0(\mathcal{K})},\end{cases} \quad (11)$$

where $g_{v,k}$ is the kth fading envelope of Q; $I_0(\cdot)$ is the zero-order modified Bessel function of the first kind, $\theta_p \in [-\pi, \pi)$ accounts for the average direction of AOA of scattering components, and $\mathcal{K} \geq 0$ represents the width of AOA of scattering components. According to the previous assumption given in the first footnote, the distributions of AOAs, θ_p and $\mathcal{K}$, are similar at the identical position.

By using the previous assumption, we thereby have a better approximation in time domain given by

$$\underbrace{\lim\phi_{g_{k,u}g_{k,u}}(\tau_u)}_{v\to u:\{f_{D,u}\to f_{D,v}\cap\tau_u\to\tau_v\}}=\phi_{g_{k,v}g_{k,v}}(\tau_v). \quad (12)$$

Thus, the master vehicle P_u and i cooperative vehicles $\left\{Q_v^1, Q_v^2, \cdots, Q_v^i\right\}$ have the same channel statistics. The upcoming estimate $\widehat{h}(x_{u+1}, y_{u+1}; \tau)$ can thus be refined from a set of historical observations h_u and $\mathbf{h}_v^i$.

Second step: For each observation at master vehicle P_u and cooperative Q_v, the initial channel estimate $\widehat{\mathbf{h}}(n,k)$ with LMMSE criterion is given by

$$\hat{\mathbf{h}}(n,k)=\mathbf{R}_{\hat{\mathbf{h}}\hat{\mathbf{y}}}\mathbf{R}_{\hat{\mathbf{y}}\hat{\mathbf{y}}}^{-1}\hat{\mathbf{y}}, \quad (13)$$

where $y \in \hat{\mathbf{y}}$ is a pilot vector used to estimate the channel $h(k)$ at epoch k, and the channel estimate is obtained using (2a) as $y = r(t)/\tilde{S}(t-\tau)\ \ ,\ \forall\, u, v$; $\mathbf{R}_{\hat{\mathbf{h}}\hat{\mathbf{y}}}$ is the correlation vector between $\hat{\mathbf{h}}(n,k)$ and $\hat{\mathbf{y}}$; $\mathbf{R}_{\hat{\mathbf{y}}\hat{\mathbf{y}}}^{-1}$ is the auto-correlation matrix of vector $\hat{\mathbf{y}}$. Clearly, (13) is only applicable under the quasi-static channel condition [8].

Based on the above derivation, let $h_u, \mathbf{h}_v^i \in \hat{\mathbf{h}}(n,k)$ be the time and spatial related observations, where the observation vector is $\left\{h_u(n,k), h_v^1(n,k), h_v^2(n,k), \cdots, h_v^j(n,k)\right\}$. Thus, the cross-correlation matrix $\mathbf{r}_{uv}$ between $h_u(n,k)$ and $h_v(n,k)$ can be represented as

$$\mathbf{r}_{uv}=\mathbf{xcorr}_{uv}=\mathbf{E}\left\{h_u(n,k)h_v^*(n,k)\right\}\quad \forall\, u, v, \quad (14)$$

where $r_{ij}(x_i, y_i; x_j, y_j) \in \mathbf{r}_{uv}$ is the cross-correlation variation related to the positions of the ith P and the jth Q. Therefore, for the upcoming estimates $\widehat{h}_{u+1}$ and its spatial related historical observations, it can be seen that upcoming estimation of $\widehat{h}_{u+1}$ is mathematically tractable by multi-user measurements h_u and $\mathbf{h}_v^i$. Now, $\widehat{h}(x_{u+1}, y_{u+1}; \tau)$, the optimal estimation $\widehat{h}_{u+1}(n,k)$ can be determined by interpolation operator $\mathbf{\Phi}$ from the following j cooperative observations ($j < i$), in which the optimal set $\mathbf{h}_v^j$ ($j = 1, 2, \cdots$) is constrained by Υ via

$$\begin{aligned}&\text{maximize}\ \ \mathbf{h}_v^j=\left\{h_v^1\cdots h_v^i\right\}\Big|_{\|Q_v^i-P_{u+1}\|\leq\Upsilon}\quad j\leq i\\ &\text{subject to}\ \ \widehat{h}_{u+1}(n,k)=\mathbf{\Phi}\left[h_u(n,k), h_v^1(n,k)\cdots h_v^j(n,k)\right].\end{aligned} \quad (15)$$

III. IVC-CE USER COOPERATION MECHANISM

The main idea of IVC-CE is that the impact of imperfect channel estimation in high-mobility scenarios can be alleviated by a set of time and spatial related observations. In this section, we formulate a mechanism of cooperation user selection to make IVC-CE available in a practical vehicle environment, where the key solution is to incorporate user position and velocity information as a priori knowledge. We thereby proposed a method to select appropriate cooperative users, where a single or multiple observations can be utilized to mitigate the impact of imperfect CSI. As described in (6), IVC-CE requires position and speed information, and therefore cooperative user selection should base on location-aware, which involves the acquirement and processing of a priori knowledge, e.g., vehicle position and velocity. In this regard, the ideal inter-vehicle cooperation may occur when the master vehicle and its cooperative vehicles have a steady motion state. It also means that all vehicles involved in cooperation should maintain the same direction and velocity within a limited cooperation scope.

Let us look at a realistic vehicular environment, for example, highways, urban streets, suburban streets and rural streets. Obviously, there is always a certain vehicle density on the road, and the vehicle density varies over time and space. In most instances, there are many opportunities for vehicle cooperation on roads, especially on highways and city streets. We focus on solving three key technical issues in this work: 1) Potential cooperative user identification; 2) optimal cooperative user selection; 3) robust user tracking. Because the high-mobility communications are mainly of interest in this paper, we will only consider a typical highway scenario in the following analysis throughout this paper. Firstly, in order to constitute the vehicle cooperation mechanism, we propose a 2-D one-way freeway model, where

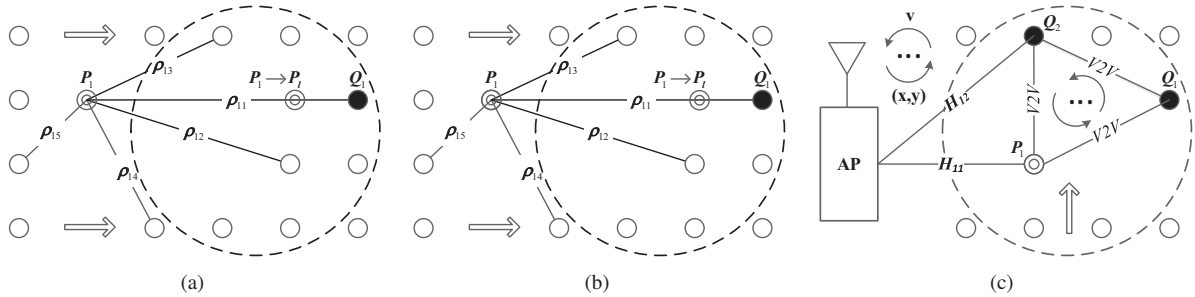

Fig. 2. Snapshot of inter-vehicle cooperation: user selection and information exchange, where vehicles are represented by circles: (a) Single-user selection with 7 candidates, (b) multi-user selection: 3 cooperative users, and (c) message exchange: request and broadcast etc.

there are multiple lanes and vehicles moving in the same direction.

Fig. 2 shows a snapshot of inter-vehicle cooperation in a 4-lane one-way road, where the arrow represents the direction of travel. Single-user selection, multi-user selection and vehicular information exchange are illustrated in Figs. 2(a), 2(b), and 2(c), respectively. For simplicity, we do not consider the impacts of the traffic model on vehicular mobility, because it has little effect on our problem formulation. However, if necessary, standard Markovian assumptions could be applied to describe the approximate traffic statistical characteristics [30].

As shown in Figs. 2(a) and 2(b), we consider a scenario where the master vehicle has a chance to cooperate with neighboring vehicles through a simple user selection mechanism. The goal is to identify one or more vehicles to perform joint channel estimation. To proceed with our analysis, let d be the distance between the ith master vehicle and the jth candidate cooperative vehicle, and v_P^i and v_Q^j are the corresponding speeds.

In order to select the cooperative vehicles from the candidate vehicles, we first define a parameter ρ_{ij} to identify the movement similarity between the ith vehicle and the jth vehicle.

Definition 1: The vehicle connectivity coefficient ρ_{ij} is a normalized ratio to illustrate the movement similarity among different vehicles, and can be expressed as

$$\rho_{ij} = \begin{cases} 1 - \frac{\left|v_P^i - v_Q^j\right|}{\mathbf{MAX}\{v_P^i, v_Q^j\}} & v_P^i \neq 0 \\ 0 & v_P^i = 0. \end{cases} \tag{16}$$

By using (16), ρ_{ij} is used to identify the movement similarity of the ith master vehicle and the jth candidate vehicle, shown in Figs. 2(a) and 2(b). In the next step, we can see that the direction of movement can be determined by some location-aware techniques (see **Remarks 1** infra).

Definition 2: The effective inter-vehicle cooperation distance d_{CO} is a limited range between the master vehicle and the cooperative vehicle, and it is defined by

$$d_{CO} = \|P_v - Q_u\|, \quad d_{\min} \leq d_{CO} \leq d_{\max}, \tag{17}$$

where $d_{\min}$ and $d_{\max}$ are the minimum and maximum cooperation distances. This relation indicates that the transmission time is bounded by the inter-vehicle cooperation. To avoid ambiguity, we emphasize: 1) $d_{\max}$ is not the range of the fixed scattering area; 2) It is the historical observations rather than the vehicles which are located in an identical scattering environment, and the historical observations for IVC-CE can be determined under the distance constraint Υ.

To select the best cooperative vehicles among all candidate vehicles, the user selection criterion must satisfy (17) and $\varepsilon \leq \rho_{ij} \leq 1$. Here, we denote ε as an acceptance minimum threshold that is used to select the desired cooperative user. According to a pre-set threshold, we can obtain the trustworthy cooperative vehicles set, say $\{\rho_{11}, \rho_{12}, \rho_{13}\}$, from a group of observed data $\{\rho_{11}, \rho_{12}, \rho_{13}, \rho_{14}, \rho_{15}\}$, as shown in Fig. 2(b).

From (16) and (17), we can derive an effective inter-vehicle cooperation time T_{CO}, a maximum duration time, with which the cooperation between P and Q can be maintained. For simplicity, assuming v_P^i and v_Q^i to be constants, we can then denote d_0 as the initial distance between P and Q. Consequently, T_{CO} can be approximated by

$$T_{CO} = \begin{cases} (d_{\min} - d_0)/(v_P^i - v_Q^j) & v_P^i > v_Q^j \\ (d_{\max} - d_0)/(v_Q^i - v_P^j) & v_P^i < v_Q^j \\ \infty & v_P^i = v_Q^j. \end{cases} \tag{18}$$

As shown in Fig. 2(c), we further detail the cooperative user searching and message transmission mechanisms. The operation of IVC-CE mode are summarized as follows:

Step 1) The master vehicle P initializes the cooperation request by transmitting an uplink message MSG_{REQ}^P to the AP. This message contains the current position (x_1, y_1) and the speed v_p^1 of the master vehicle.

Step 2) Once the AP receives MSG_{REQ}^P, it immediately generates a downlink broadcast message MSG_{BCCH} constituted by the master vehicle's position, speed and the pre-defined minimum threshold ε. In this case, MSG_{BCCH} is sent in the broadcast control channel (BCCH) to all receivers.

Step 3) After receiving MSG_{REQ}^P, the receivers begin to calculate ρ_{ij} and d_{CO}. If there are one or more current calculated results that meet (18), the corresponding receivers are considered as candidate cooperative vehicles. Next, candidate vehicles immediately respond their positions and speeds to the AP by an uplink response message MSG_{RES}^Q.

Step 4) The AP is responsible for assigning tasks to these selected cooperative users and performing the IVC-CE process. The results of the assignment are broadcasted to the vehicle receivers in the BCCH. The measurement involving single or multiple cooperative vehicles is simultaneously triggered by the AP broadcast instruction message MSG_{BCCH}^{sys}.

Algorithm 1 Calculate the distance of the inter-vehicle cooperation, identify the set of cooperative users, and set up a virtual connection relationship between the master vehicle and the cooperative vehicles.

procedure COOPERATIVE USER SELECTION (P_u, Q_v, ρ_{ij})
  Initialization ($d_{\min}$, $d_{\max}$, MSG, ε, $\cdots$)
  $MSG^{P}_{REQ} \rightarrow AP$
  for all Q_v **do**
    if $\rho_{ij} \geq \varepsilon$ **then**
      $MSG^{Q}_{RES} \rightarrow AP$
    end if
  end for
  select co-user **trigger** IVC-CE $AP \rightarrow MSG^{sys}_{BCCH}$
  repeat
    $MSG^{sys}_{REQ} \rightarrow AP$
    if count(Q_v) $\neq 0$ **then** continue
    else $MSG^{P}_{REQ} \rightarrow AP$
    end if
  until interruption condition is **true**
end procedure

procedure INTERRUPT OF STEERING ANGLE (θ_{st})
  if $\theta_{st} \in P$ **then**
    $MSG^{P}_{reset} \rightarrow AP$ ▷ release current cooperation
  else if $\theta_{st} \in Q$ **and** count(Q_v) $\neq 0$ **then** continue
  else $AP \rightarrow MSG^{Q}_{reset}$
  end if
end procedure

Step 5) The AP periodically broadcasts the system message MSG^{sys}_{REQ} (e.g., 10 s~30 s) to collect the mobility state information from the cooperative vehicles and conveys the related information to the next AP.

Remarks. 1 In steps 1, 3, and 5, we assume that each vehicle knows its position and velocity. In fact, the position, speed and direction can be acquired by low-complexity real-time techniques with on-board vehicle sensors. For example, the motion direction and speed can be obtained from *steering wheel angle sensors* and *wheel speed sensors*, and the vehicle position can be collected by a high-accuracy GPS receiver, or a network-assisted positioning technique [31].

Remarks. 2 Fig. 2(c) also illustrates an optional cooperative user selection scheme, where the master vehicle is able to communicate with its direct neighbors or other remote vehicles. In this case, the master vehicle broadcasts the cooperation request MSG_{REQ} over a V2V channel to its direct neighbor, which also has the corresponding GPS and velocity information.

The inter-vehicle cooperative user selection algorithm is outlined in **Algorithm 1**. Note that, the algorithm is adaptive and is able to track dynamic variations of cooperative users. The algorithm consists of two parts: cooperative user selection and cooperative process interruption. The interruption will occur when a large steering angle is detected.

At this point, we have described the IVC-CE model and introduced an easy-to-implement user cooperation scheme in practical vehicle scenarios. In the next section, we will use the IVC-CE method to design an optimized channel estimator and mitigate the outdated CSI problem.

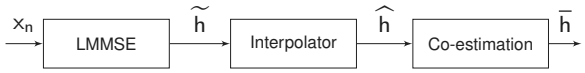

Fig. 3. IEEE 802.11p channel estimation scheme.

IV. IVC-CE FOR SAFETY RELATED DATA TRANSMISSION

In this section, we discuss a safety related data transmission scheme based on the IVC-CE model. Fig. 3 illustrates the block diagram of our proposed channel estimation scheme. In the following derivation, we will sequentially obtain $\widetilde{h}$ at the pilot positions and $\widehat{h}$ at the data positions, and more accurate $\overline{h}$ from single/multi-user cooperation. Firstly, the LMMSE estimator and linear interpolation algorithm are employed to obtain the static channel estimates at the pilot and data positions [8], [9], [26]. Secondly, a linear interpolation estimation approach performed by single or multi-user cooperation is developed, resulting in an accurate channel estimate, and the impacts of outdated CSI are thereby mitigated. Finally, we design a scalable transmission scheme to support the safety related data applications.

A. Quasi-Static LMMSE Channel Estimation Scheme

OFDM channel estimation techniques have been extensively studied in the literature [4]–[14]. For channel estimation in time domain, the mean squared error (MSE) criterion is widely adopted to evaluate the performance of various channel estimators, which is expressed by

$$\mathrm{MSE} = \mathrm{E}\left\{\frac{1}{K}\sum_{k=1}^{K}\left|\widetilde{h}(n,k) - h(n,k)\right|^2\right\}, \tag{19}$$

where $\widetilde{h}(n,k)$ is the channel estimate of the kth subcarrier at the nth OFDM symbol position [9]. Then, the estimated CIR at the pilot positions can be expressed as

$$\widetilde{h}_P(p,q) = h_P(p,q) \; + \; e(p,q), \tag{20}$$

where $e(p,q)$ is the estimation error that is statistically independent from $h_P(p,q)$.

Generally, optimum channel estimator design requires the channel statistical knowledge, such as the correlation matrices in time and frequency domains. To obtain the estimation of the channel knowledge at data symbol positions, the 1-D/2-D interpolation methods are necessary in both of time and frequency domains, e.g., linear interpolation, second-order interpolation, low-pass interpolation and spline cubic interpolation. For example, a typical MMSE interpolation estimator is considered in [26], which employs the second-order statistics of the channel to minimize the mean-square error. In Subsection IV-B, we will investigate an efficient interpolation method that considers historic observations.

For master vehicles, the LMMSE algorithm can be written as

$$\widetilde{\mathbf{h}}_{u,LMMSE} = \mathbf{R}_{h_u\widetilde{h}_u}(\mathbf{R}_{\widetilde{h}_u\widetilde{h}_u} + \frac{\beta_u}{snr_u}\mathbf{I}_u)^{-1}\mathbf{h}_{u,LS}, \tag{21}$$

where $\widetilde{h}_u$ is the CIR at the pilot subcarriers; $\mathbf{h}_{u,LS}$ is the initial channel estimation carried out by using the least square (LS) algorithm; $\mathbf{R}_{h_u\widetilde{h}_u}$ represents the cross-correlation between all the subcarriers and the pilot subcarriers, and $\mathbf{R}_{\widetilde{h}_u\widetilde{h}_u}$ represents the auto-correlation matrix among the pilot subcarriers [5]. Here, $\mathbf{I}_u$ is an identity matrix; $snr_u = E(x_{u,i}^2)/\sigma_{u,n}^2$ is the average SNR, and $\beta_u = \mathrm{E}(x_{u,i}^2)\mathrm{E}(1/x_{u,i}^2)$ is a constant determined by the constellation point $x_{u,i}$. Since the SNR and the channel correlation matrix $\mathbf{R}_{\widetilde{h}_u\widetilde{h}_u}$ will be estimated in (14), the LMMSE algorithm still has a high computational complexity so that it may not be feasible for implementing in practice.

To further reduce the computational complexity, an optimal LMMSE method based on singular value decomposition (SVD) is proposed [8]. In general, the auto-correlation matrix $\mathbf{R}_{\widetilde{h}_u\widetilde{h}_u} \in \mathbb{R}^{m\times m}$ is a Hermitian matrix, and $\mathbf{R}_{\widetilde{h}_u\widetilde{h}_u}$ can thus be decomposed according to the SVD method by

$$\mathbf{R}_{\widetilde{h}_u\widetilde{h}_u} = \mathbf{U}\mathbf{\Lambda_u}\mathbf{U}^{\dagger} \quad \in \mathbb{R}^{m\times m}, \tag{22}$$

where the matrix $\mathbf{U}$ is orthonormal and $\mathbf{U} \in \mathbb{R}^{m\times m}$; $\mathbf{U}^{\dagger}$ is the Hermitian transpose of $\mathbf{U}$ and $\mathbf{\Lambda_u}$ is an $m \times m$ diagonal matrix with positive eigenvalues λ_k in descending order, such that $\lambda_0 \geq \lambda_1 \geq \cdots \geq \lambda_k > \lambda_{k+1} > \cdots > \lambda_{m-1} = 0$. Then, substituting (21) into (22) yields

$$\widetilde{\mathbf{h}}_{u,LMMSE} = \mathbf{U}(\mathbf{diag}[\delta_{u,i}])\mathbf{U}^{\dagger}\mathbf{h}_{u,LS}, \tag{23}$$

where $\delta_{u,i} = \lambda_i/(\lambda_i + \beta_u/SNR_u)$, $i = 0, 1, \cdots, m-1$.

By observing (21), as long as the receiver is in IVC-CE operation mode, it should be emphasized that the β_u and SNR_u in (21) can be replaced by β_v and SNR_v, respectively. This can be achieved by using a priori statistical knowledge from the cooperative vehicles. It can be explained by the fact that the statistics of the master vehicle and its cooperative vehicles are highly correlated. Therefore, the channel statistics of the vehicles in the same cooperation set can be reused for the master vehicle. For this reason, additional benefits are that incomplete CSI (even lost) could be restored when impulsive noise, interference and/or calculation error occurs. As a result of such a restoration mechanism, the accurate CSI at the transmitter can be further guaranteed.[3]

B. Kinematic User Cooperative Estimation Scheme

In this subsection, we develop an effective interpolation estimation method to mitigate the effects of the delay or outdated CSI in high-mobility IEEE 802.11p systems. For a specific pilot pattern in the OFDM time-frequency grid, channel estimation at the data positions can be obtained by choosing a set of interpolation basis functions. Given a set of pilot-aided channel estimates $\left\{\widetilde{h}_u(p,q)\right\}$, the CIR at the data position $\widehat{h}_u(n,k)$ can thus be obtained by neighboring pilot estimates via

$$\widehat{h}_u(n,k) = \sum_p \sum_q \mathbf{\Phi}\left(\widetilde{h}_u(p,q)\right), \tag{24}$$

[3]The alternative solution of the above algorithm may also be normalized least mean squares (NLMS) and recursive least squares (RLS) algorithms [9].

where $\mathbf{\Phi}$ is a set of interpolating base-functions $\{\Phi_1, \Phi_2, \cdots, \Phi_n\}$, and W_j is the weighting coefficients [26]. By choosing different interpolating base-functions, e.g., linear, spline, and Gaussian filters, the estimates $\widehat{h}_v(n,k)$ at all subcarriers can be obtained. Several efficient interpolation techniques for pilot symbol-assisted channel estimation in OFDM systems have been compared for the case of 2-D separable Wiener filter. This interpolation architecture has been proved to be equivalent to the 1-D and 2-D MMSE interpolation and can provide better performance with low complexity [26], [27].

In [12], it has verified that multiple estimates from different frequencies or time slots can enhance the performance and tolerate larger errors in channel estimation. This paper further points out that multiple spatial related observations are available to yield accurate up-to-date channel estimation results. As a result, the upcoming estimate $\widehat{h}_{u+1}(n,k)$ can be fitted by a set of historical measurements, which is calculated by a general discrete interpolation filter given by

$$\widehat{h}_{u+1}(n,k) = \sum_{n=0}^{N-1} w_n(k)\widehat{h}_v^j(n,k), \tag{25}$$

where N is the number of subcarriers. Here, $\widehat{h}_v^j(n,k) = \left\{\ \widehat{h}_u(n,k) \quad \widehat{h}_v^j(n,k)\ \right\}$ is the spatial related channel estimate set at pilot positions. Additionally, the cross-correlation matrix is predefined as $\mathbf{r}_{uv}$, and the normalized cross-correlation function for non-isotropic scattering environment can be represented as $r_{uv} = \mathrm{E}[h_u h_v^*]\Big/\sqrt{\Omega_u\Omega_v}$, where Ω_u and Ω_v are the received signal power at the measurement positions u and v, respectively [19]. The detailed derivation of the multi-link cross-correlation function and the correlation coefficient can be found in [21] and [22].

Generally, the MMSE interpolation algorithm chooses appropriate filter coefficients to achieve the MMSE solution by $\mathrm{MMSE}\big|_{w_n(k)} = \min\left(\mathrm{E}\left[\left|\widehat{h}(n,k) - h(n,k)\right|^2\right]\right)$ [26]. By using Wiener filter, the interpolation in time domain can be achieved by

$$\mathbf{w}_n = (\mathbf{R}_{\widehat{h}_v^j\widehat{h}_v^j} + \frac{N_0}{E_s}\mathbf{I})^{-1}\mathbf{R}_{h_v^j\widehat{h}_v^j}, \tag{26}$$

where the coefficients $\mathbf{w}_n$ can be calculated by Wiener-Hopf equation, given by $\mathbf{w}_n = \mathbf{R}_{h_v^j\widehat{h}_v^j}\left(\mathbf{R}_{\widehat{h}_v^j\widehat{h}_v^j}\right)^{-1}$. By repeating the derivation in [26], the channel estimate $\widehat{\mathbf{h}}_{u+1}(n,k)$ and $\widehat{\mathbf{H}}_{u+1}(n,k)$ in time and frequency dimensions can be represented as

$$\widehat{\mathbf{h}}_{u+1}(n,k) = [\mathbf{w}_n]^H\widehat{\mathbf{h}}_v^j(n,k) \tag{27a}$$

$$\widehat{\mathbf{H}}_{u+1}(n,k) = [\mathbf{W}_n]^H\widehat{\mathbf{H}}_v^j(n,k), \tag{27b}$$

where $\mathbf{W}_n$ is the filter coefficients in the frequency dimension. As shown in the above derivation, it is highly possible that the master vehicle and its cooperative vehicles will share similar channel statistics within a certain range. Even if there is incomplete or outdated CSI, it is still possible to obtain up-to-date CSI at the master vehicle receiver.

C. Scalable Data Transmission Scheme

In Section II, we have introduced a MMSE interpolating method to obtain the channel estimates at data positions, which

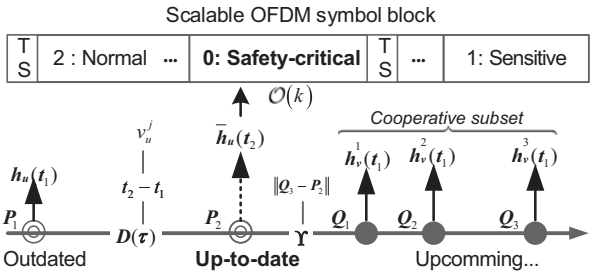

Fig. 4. OFDM scalable data transmission at the physical layer.

cannot only improve the accuracy of channel estimation, but also simplifies channel estimation by using a priori knowledge of cooperative vehicles. However, it is still not the optimal estimator, because the up-to-date estimates would quickly become outdated in high-mobility environments. According to the low-latency requirement of emergency communications, we subdivide the vehicular data transmission into the categories of normal, sensitive and safety related transmissions [2]. To support safety related applications in VANETs, e.g. collision alert, merge assistance, road condition warning, more reliable data transmission is worth taking into account. Next, we aim to find out the optimal OFDM symbol transmission to provide safety related data applications, and the key point is that the optimal transmission time slot should be chosen in terms of the best channel estimates.

Fig. 4 illustrates the key elements of the optimal channel estimation, which enables a scalable data transmission at the physical layer. Here, a simplified 1-D vehicle motion model is taken into account under the highway scenario. It is supposed that the channel statistics of one master vehicle and three cooperative vehicles have been determined. Clearly, the channel estimation $h_u(t_1)$ is outdated owing to vehicle motion. From (15), the optimal estimation $\overline{h}_u(t_2)$ would be interpolated by a set of cooperative observations, e.g., $h_v^1(t_1)$, $h_v^2(t_1)$, and $h_v^3(t_1)$.

In order to mitigate the outdated CSI problem caused by transmission and/or computation delay, a definition of the optimal OFDM data transmission time slot is required. We thereby stipulate:

Definition 3: The optimal OFDM data transmission time slot $O(\chi)$ is bounded below by two delay constraints

$$\mathcal{T}_{\max} \le O(\chi) < \mathcal{T}_{p,q}, \tag{28}$$

where χ is the total delay variant and $\mathcal{T}_{\max}$ denotes the maximum allowed delay including computation and feedback delay; $\mathcal{T}_{p,q}$ denotes the constraint on the maximum time interval such that the master vehicle P moves from its current position to the position of cooperative vehicle Q. Suppose that the channel response is short-term stationary, which implies the feasibility of the estimation with the constraints on $O(\chi)$. Accordingly, as shown in the Fig. 4, $O(k)$ denotes the kth desirable OFDM symbol block, and it also represents an optimal channel estimation condition for safety related data transmission.

Based on this definition, the main objective in the next part is to find the most efficient way to choose the transmission time. From the resultant optimal $O(k)$, the optimal transmission time for a particular safety related data transmission can be obtained. It should be noted that the optimal OFDM data transmission time $O(k)$ is not a randomly chosen time slot, and the system processing delay would be negligible. Hence, the optimal strategy for scalable transmission at the physical layer is to first pre-calculate the channel estimate at the next position, and once the accurate estimate $\overline{h}_{u+1}(t_1)$ is obtained, it can be viewed as an up-to-date channel estimate. As a result, there is no outdated channel estimate, while the transceiver waits for the channel estimate to be refined.

Now the outdated estimation is ready to be refined by applying the IVC-CE technique. For a set of historical channel estimates $\{\widehat{h}_u(t_n), \widehat{h}_v^1(t_n), \cdots\}$, at time t_n, it is assumed that all channel estimates at the pilot and data symbol positions have been evaluated. Let $T_{\text{opt}} = t_n + \chi_{\max} + nT_{SB}, n \in \mathbb{N}$ be the expected transmission time with maximum delay related $\chi_{\max}$. For simplicity, we consider a simplified polynomial fitting approach - linear interpolation algorithm given in (7), which involves historic observation $\widehat{h}_v^1$ and $\widehat{h}_v^2$. Then, the up-to-date estimates $\widehat{h}_{u+1}$ is finally updated by

$$\begin{aligned} &\text{minimize} \quad \Upsilon = \left\| P_{u+1} - Q_v^j \right\|, \forall Q_v^j, j = 1, 2, \cdots \\ &\text{subject to} \quad \overline{h}_{u+1}(T_{opt}) = \widehat{h}_v^1 + \frac{\|P_{u+1}\| - \|Q_v^1\|}{\|Q_v^2\| - \|Q_v^1\|} \widehat{h}_v^2, \end{aligned} \tag{29}$$

where $\overline{h}_{u+1}(T_{opt})$ denotes the channel estimate at time T_{opt} in terms of the current position. According to **Definition 3**, the delay-constrained problem can satisfy the requirements given in (28), which produces its expression given by $t_n + \chi + nT_{SB} : [\mathcal{T}_{\max}, \mathcal{T}_{p,q}]$. In order words, if the processing delay is assumed to be less than six OFDM symbols, then the expected transmission time slot can be given by $T_{\text{opt}} = \chi_{\max} + 6T_{SB}$. Additionally, if there are multiple alternate transmission time slots, the time slot with the maximum signal-to-noise can be regarded as ideal. Consequently, for the current estimate $\overline{h}_{u+1}$, it's mapping to the kth OFDM symbol can be expressed by

$$\begin{aligned} &\text{minimize} \quad \tau + nT_{SB} : O(\chi) \to O(k) \\ &\text{subject to} \quad T_{\text{opt},} \end{aligned} \tag{30}$$

where $O(k)$ denotes the optimal time slot for safety related data transmission. Once the optimal transmission time slot$O(k)$ is determined, then, a particular time slot T_{opt} can be selected by (30) to support burst data transmission. In this case, the CIR of all subcarriers should be computed in the $(n + k)$th OFDM symbol if required. Similarly, channel estimates at data positions can be fitted by previous interpolation method.

Based on the proposed method, it is possible to acquire accurate up-to-date CSI and tolerate large CSI latencies during V2I communication process. As a result, the scalable data transmission would be helpful to improve the performance of safety related applications. If necessary, the proposed method could be combined with other interpolation algorithms, e.g., cubic high order fitting and polynomial fitting [27]. The preliminary transmission control algorithm of the scalable data transmission at the physical layer is presented in **Algorithm 2**.

Algorithm 2 Physical layer scalable transmission and symbol block mapping.

procedure OFDM SCALABLE TRANS ($\mathcal{T}_{\max}$, $\mathcal{T}_{p,q}$)
  $X_n \rightarrow \widetilde{h} \rightarrow \widehat{h}$ ▷ initialization
  while $O(\chi)$ **do** ▷ optimal transmission time
    $P \leftarrow Q$ ▷ user cooperation
    $\overline{h}_{u+1} \leftarrow \Phi\left\{\widehat{h}_u, \widehat{h}_v^1, \widehat{h}_v^2 \cdots\right\}$ ▷ interpolation
    $T_{\text{opt}} \leftarrow \tau_{\max} + nT_{SB}$
  end while
  return k ▷ optimal symbol block mapping k
end procedure

Table 2. IEEE 802.11p Simulation Parameters.

Parameters	Descriptions	Values
N	Number of training symbols	8,192
R_b	Data rate	3 Mbits/s
N_D	Number of data subcarriers	48
N_P	Number of pilot subcarriers	4
T_{Signal}	Duration of the OFDM symbol	8 μs
T_G	Guard time	1.6 μs

V. NUMERICAL RESULT

In this section, the performance evaluation of IVC-CE is carried out by extensive simulations, where different parameter settings and mobility conditions are considered. This paper focuses on the V2I communications operating at the 1,400 MHz frequency band, which is planning to be identified as an industrial and public safety radio band in China. In some cases, the frequency band 1,375–1,400 MHz and 1,427–1,452 MHz is being considered for the mobile service [32]. The simulation parameters of IEEE 802.11p physical layer are summarized in Table 2.

The V2I channel model can be regarded as a special V2V channel, where the antenna height of the AP is raised up, and a stationary scattering environment is supposed. Particularly, the time-selective fading statistics of V2I communication links substantially differ with cellular communication networks [33]. Therefore, existing geometry-based statistical channel models (GSCMs) are more suited for non-stationary environments and have advantages especially when node movement needs to be simulated [33]–[36]. Thus, it can be applied to fixed-to-mobile (F-to-M) channels with a slight modification. In our simulations, we adopt a geometry-based statistical model (GBSM) for non-isotropic F-to-M Ricean fading channels in both macro- and micro-cell scenarios, where the phase may not be uniformly distributed in non-isotropic scattering environments [35]. For simplicity, we approximate the V2I radio propagation in highway environments by a 2-D non-isotropic scattering model with LOS and single-bounced component conditions between the Tx and Rx:

$$\hat{h}^{(A-V)}(n\Delta t_s, k\Delta\tau_s) = \hat{h}^{(LOS)}(n\Delta t_s, k\Delta\tau_s) + \hat{h}^{(SB)}(n\Delta t_s, k\Delta\tau_s). \tag{31}$$

To obtain the theoretical values of the system function, we perform the fast Fourier transform (FFT) over 500 snapshots for the predefined variables t and f. It can be further observed that

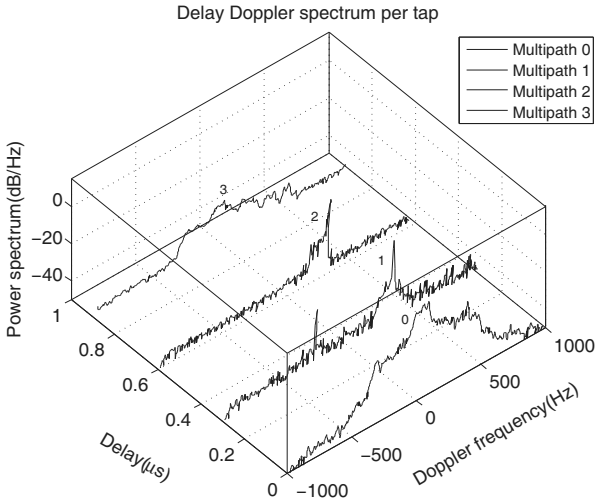

Fig. 5. Channel emulator setup for 4-multipath components: A measurement of delay-Doppler spectrum with a speed of 25 m/s.

the maximum delay resolution in time and frequency domain is determined by $t_{\max} = [1/(B_d\Delta t_s)]$ and $f_{\max} = [1/(\Delta f_s\tau_{\max})]$, respectively. B_d is the Doppler spread and $\tau_{\max}$ is the maximum relative delay. Fig. 5 illustrates an experimental statistics of the delay-Doppler spectrum in our channel emulator setup, in which the local scatterers are randomly deployed around the vehicle receivers, according to the nonuniform distribution for AOAs. The power spectral density is produced by averaging 5,000 snapshots, and a widening of the Doppler spectrum exhibits the LOS-like behavior (aka Ricean behavior). Firstly, we use the EB (Elektrobit) Propsim C8 radio channel emulator to create the V2I channel model. The dynamic impulse response data are generated by the C8 channel emulator, which are employed to compute the delay spread and Doppler spread. Then, the proposed IVC-CE scheme can be simulated according to the LMMSE algorithm, where the correlation matrices are available from the impulse response data. To obtain accurate fading correlation information automatically in vehicular communication scenarios, we set the parameters of multipath components (MPCs) to adapt the changes of the direction of departures (DOAs), direction of departures (DODs), and delays due to large-scale movements of the vehicle receivers. Additionally, we also consider the correlation between the DOAs and the Doppler shift for the vehicle receiver. To simultaneously utilize the channel measurements of delay spread and Doppler spread statistics, we set the delay resolution $\Delta\tau_s = 4$ ns, sampling period $\Delta t_s = 100$ us, and the maximum delay spread and maximum Doppler spread are set to be 744 ns and 1361 Hz, respectively [37]. Additionally, the model parameters B_d and $\tau_{\max}$ can also be configured from the measured space Doppler power spectral density (sD-psd) and the power space-delay spectral density (psds) if the measurement data could be obtained by channel-sounding experiment conducted in practical scenarios.

A. Channel Estimation Performance

Figs. 6 and 7 show the IVC-CE performance in terms of MSE versus BER and compare it with the traditional LMMSE al-

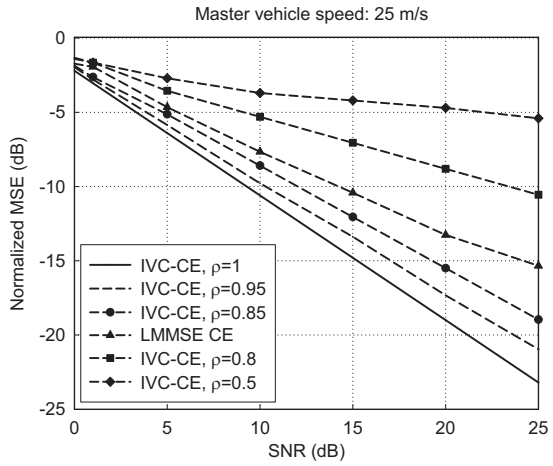

Fig. 6. IVC-CE performance: normalized MSE vs. SNR. There are a master vehicle P and a cooperative vehicle Q. The distance between the AP and P $\|P_u\| = 200$ m. The distance between P and Q is set as $\Upsilon = 0.5$ m.

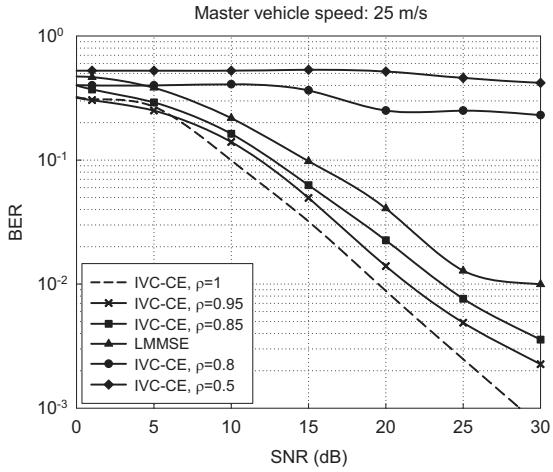

Fig. 7. IVC-CE performance: BER vs. SNR. There are a master vehicle P and a cooperative vehicle Q. The distance between the AP and P $\|P_u\| = 200$ m. The distance between P and historical Q is set as $\Upsilon = 0.5$ m.

gorithm. The normalized MSE is characterized by a complex Gaussian random variable with zero mean and a variance σ_e^2. The MSE and BER performance is simulated with different IVC-CE conditions that are associated with the vehicle connectivity coefficient ρ_{ij}. Figs. 6 and 7 illustrate that with an increasing vehicle connectivity coefficient ρ_{ij} improves, the MSE estimation and BER performance are improved. It can be observed that $\rho_{ij} \geq 0.85$ is sufficient to support IVC-CE operation.

To further demonstrate the effectiveness of IVC-CE, Fig. 8 shows the estimation performance of IVC-CE at different vehicle speeds (30 km/h, 90 km/h, and 120 km/h), where the effects of different ρ_{ij} at high speed and low speed conditions are investigated. By comparing the results given by different vehicle connectivity coefficients ρ_{ij}, some crucial properties of the proposed system can be revealed. In high speed scenarios (25~33 m/s), we observe that the estimation performance is significantly affected by ρ_{ij}. As illustrated in Figs. 8(a) and 8(b), when $\rho_{ij} \leq 0.5$, the performance degradation becomes severe and multi-user cooperation cannot provide performance improvement, similar to the results in Fig. 6. In the low speed scenario (8.3~13.8 m/s), we observe a very interesting phenomenon. Whatever ρ_{ij} is large or small, the channel estimation error can be reduced by multi-user cooperation and achieve better BER performance. This result is obviously useful in complex urban street environments, where IVC-CE will experience very different ρ_{ij}. Fig. 8(c) illustrates the CFRs interpolation results with multi-users pilots, where each user has 4 pilot subcarriers and 48 data subcarriers. We have already established a linear multi-user interpolation model in Section III, and the CFRs of the master user can be obtained at all subcarrier positions by using different interpolating approaches. Furthermore, the master user is able to make full use of the pilot source from cooperative users, and thus more pilot estimates are available to improve the system performance.

B. Mitigation of Outdated CSI Problem

In Section IV, we develop an effective method to mitigate the effect of the outdated CSI in high-mobility IEEE 802.11p environments. To verify the analysis of the method, we adopt traditional pilot-assisted channel estimation algorithm to investigate the benefit of multiple estimates. This method can be easily extended to the case when multiple estimates from both different frequencies and time slots are available. In contrast to existing methods using multiple outdated channel estimates, IVC-CE uses multiple up-to-date channel estimates that can provide additional knowledge of the fast time-varying channels to obtain more accurate channel estimates. Fig. 9(a) depicts how the number of pilot estimates affects the normalized MSE performance. As expected, by using a priori pilot statistical knowledge of the cooperative vehicles, we observe that the normalized MSE performance is significantly improved. It can also be observed that multiple introduced upcoming estimations have about 3~5 dB performance gain compared to the non-cooperation scenario where all of the pilot estimates are outdated. As one might expect, the initial performance improves quickly as the number of estimates increasing from 1 to 10, and after that, the performance improvement related to the number of estimates becomes trivial. This case can be explained in Fig. 9(b) which shows that the BER performance is not only influenced by the channel estimation error but also by the normalized cross-correlation coefficient r among different measurement sequences of vehicle P and vehicle Q. As we discussed in Section IV, the cross-correlation coefficient characterizes the specific multilink spatial correlations (instead of time or frequency correlations) in a sparse non-isotropic scattering environment. We can see that a higher spatial correlation factor can significantly improve the accuracy of channel estimation.

C. Scalable Data Transmission Performance

In Fig. 10, we simulate the BER performance for the proposed OFDM scalable transmission scheme. It is clear that the scalable transmission scheme offers the most reliable data transmission performance. Such superior performance is obtainable, since IVC-CE is able to yield the best up-to-date channel estimates.

The BERs were obtained by averaging over 100 experiments with 1,000 OFDM symbols in which the safety related data ac-

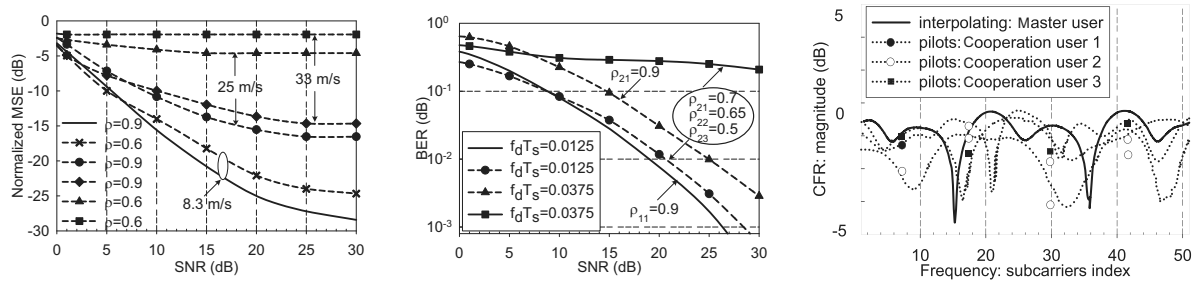

(a) (b) (c)

Fig. 8. IVC-CE estimator performance with different speed v and ρ_{ij}: v = 30 km/h, v = 90 km/h, v = 120 km/h. There are a master vehicle and multiple cooperative vehicles. The parameters are set as $\|P_u\|$ = 200 m and Υ = 1 m: (a) MSE vs. SNR, (b) BER vs. SNR, and (c) CFRs interpolation results with multi-users pilots.

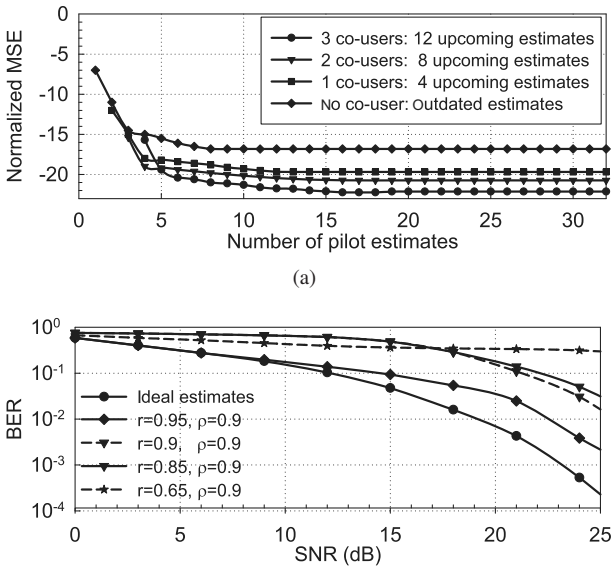

(a)

(b)

Fig. 9. Performance of multi-user pilot estimations: v = 50 km/h. There are a master vehicle and multiple cooperative vehicles. The parameters are set as $\|P_u\|$ = 250 m and Υ = 0 m, 0.5 m, 1 m, 3 m, 5 m, where Υ = 0 m refers to the ideal estimates: (a) Normalized MSE performance and (b) BER performance.

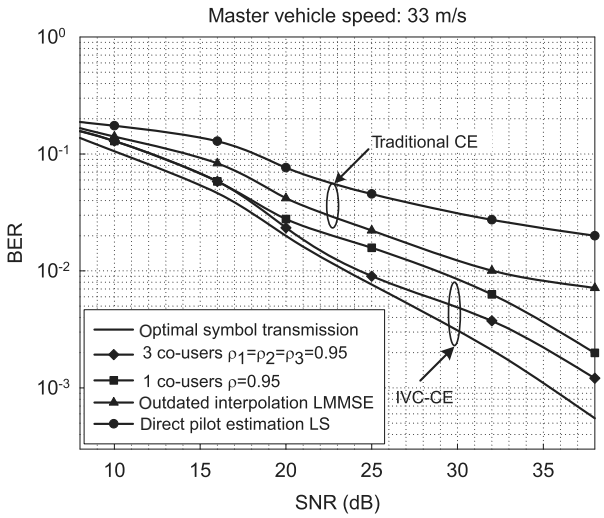

Fig. 10. OFDM scalable data transmission performance. There are a master vehicle and multiple cooperative vehicles. The parameters set as $\|P_u\|$ = 300 m and Υ = 1 m.

count for 5%. For simplicity, a complete symbol block is used to help with safety related data transmission. According to **Definition 3**, the optimal OFDM symbol transmission time can be determined from $O(\chi + nT_{SB})$, where $\chi + nT_{SB}$ is lower bounded by the maximum processing delay and must satisfy the requirements given in (21). Thus, the data burst intervals are not fixed. Once the optimal delay constraint $\chi + nT_{SB}$ has been calculated by (23). We can determine the optimal transmission T_{opt} in terms of minimum BER, and this optimal delay constraint T_{opt} can be used to obtain the closest OFDM symbol mapping $O(k)$. In this case, IVC-CE will recalculate the CIRs of all subcarriers in the $(n + k)$th OFDM symbol. As we show in Fig. 10, it is possible that multiple upcoming estimates can be used to obtain a better estimation performance. The optimal time slot for safety related transmission would wait for several OFDM symbols, and the burst data transmission can be arranged in advance. To sum up, the physical layer optimal OFDM data transmission is essential to provide different BER performance, which can be used to determine various channel estimates.

VI. CONCLUSION

This paper presented the concept of IVC-CE for IEEE 802.11p V2I communications. The main idea of IVC-CE is that imperfect CSI in a high-mobility scenario can be improved by a set of spatial related observations. The movement characteristics of the vehicle, including position and velocity, are well exploited to mitigate the impacts of incomplete and/or outdated CSI. We thereby formulated a feasible inter-vehicle cooperation mechanism to make IVC-CE an attractive and practical technique for the majority of vehicle communication environments.

Meanwhile, to further alleviate the outdated CSI problem, we developed an effective interpolation estimation method that can yield accurate up-to-date channel estimation results and support scalable data transmission at the physical layer. Simulations and numerical results show that the proposed IVC-CE technique can significantly enhance the channel estimation performance and support V2I safety related applications.

REFERENCES

[1] *IEEE 802 Standard Part 11, Amendment 6: Wireless Access in Vehicular Environments*, IEEE Standard 802.11p, 2010.

[2] U.S. Department of Transportation: DoT, Publication No. FHWA-HRT-

11-040 "Crash Data Analyses for Vehicle-to-Infrastructure Communications for Safety Applications," Tech. Rep., Nov. 2012.
[3] M. Médard, "The effect upon channel capacity in wireless communications of perfect and imperfect knowledge of the channel," *IEEE Trans. Inf. Theory*, vol. 46, no. 3, pp. 933–946, May 2000.
[4] L. J. Cimini, "Analysis and simulation of a digital mobile channel using orthogonal frequency division multiplexing," *IEEE Trans. Comm.*, vol. COM-33, pp. 665–675, July 1985.
[5] J. V. Beek *et al.*, "On channel estimation in OFDM systems," in *Proc. IEEE VTC*, July 1995, pp. 815–819.
[6] P. Hoeher, S. Kaiser, and P. Robertson, "Pilot-symbol-aided channel estimation in time and frequency," *Multi-Carrier Spread-Spectrum*, pp. 169–178, 1997.
[7] Y. Li, L. J. Cimini, and N. R. Sollenberger, "Robust channel estimation for OFDM systems with rapid dispersive fading channels," *IEEE Trans. Commun.*, vol. 46, no. 7, pp. 902–915, July 1998.
[8] O. Edfors *et al.*, "OFDM channel estimation by singular value decomposition," *IEEE Trans. Commun.*, vol. 46, no. 7, pp. 931–939, July 1998.
[9] S. Coleri *et al.*, "Channel estimation techniques based on pilot arrangement in OFDM systems," *IEEE Trans. Broadcast.*, vol. 48, no. 3, pp. 223–229, Sept. 2002.
[10] S. Zhou, B. Muquet, and G. B. Giannakis, "Subspace-based (semi-) blind channel estimation for block precoded space-time OFDM ," *IEEE Trans. signal Process.*, vol. 50, no. 5 , pp. 1215–1228, May 2002.
[11] M. K. Ozdemir and H. Arslan, "Channel estimation for wireless OFDM systems," *IEEE Commun. Surveys Tuts.*, vol. 9, no. 2, pp. 18–48, July 2007.
[12] Sigen Ye, R. S. Blum, and L. J. Cimini, "Adaptive OFDM systems with imperfect channel state information," *IEEE Trans. Wireless Comm.*, vol. 5, no. 11, pp. 3255–3265, Nov. 2006.
[13] H. Şenol, E. Panayirci and H. V. Poor, "Nondata-aided joint channel estimation and equalization for OFDM systems in very rapidly varying mobile channels," *IEEE Trans. Signal Process.*, vol. 60, no. 8, pp. 4236–4253, Aug. 2012.
[14] N. M. Idrees *et al.*, "Improving time variant channel estimation for 3GPP LTE-downlink," in *Proc. IEEE PIMRC*, 2012, pp. 2114–2119.
[15] K. Manolakis, S. Jaeckel, and V. Jungnickel, "Channel prediction by Doppler-delay analysis and benefits for base station cooperation," in *Proc. IEEE VTC Spring*, May 2013, pp. 1–6.
[16] D. J. Love *et al.*, "An overview of limited feedback in wireless communication systems," *IEEE J. Sel. Areas Commun.*, vol. 26, no. 8, pp. 1341–1365, Oct. 2008.
[17] W Bajwa, J Haupt, A Sayeed, and R Nowak, "Compressed channel sensing: A new approach to estimating sparse multipath channels," *Proc. IEEE*, vol. 98, no. 6, pp. 1058–1076, Sept. 2010.
[18] C. Oestges *et al.*, "Experimental characterization and modeling of outdoor-to-indoor and indoor-to-indoor distributed channels," *IEEE Trans. Veh. Technol.*, vol. 59, no. 5, pp. 2253–2265, June 2010.
[19] A. Abdi, M. Kaveh, "A space-time correlation model for multielement antenna systems in mobile fading channels," *IEEE J. Sel. Areas Commun.*, vol. 20, no. 3, pp. 550–560, Apr. 2002.
[20] X. Cheng, *et al.* "Cooperative MIMO channel modeling and multi-link spatial correlation properties," *IEEE J. Sel. Areas Commun.*, vol. 30, no. 2, pp. 388–396, Feb. 2012.
[21] H. Jung and M. A. Weitnauer, "Link asymmetry in virtual MISO-based networks," in Proc. *IEEE MILCOM*, San Diego, CA, Nov. 2013, pp. 1322–1327.
[22] G. Dahman, J. Flordelis and F. Tufvesson,"On the cross-correlation properties of large-scale fading in distributed antenna systems," in *Proc. IEEE WCNC*, 2014, pp. 160–165.
[23] W. C. Jakes, *Microwave Mobile Communications*, Wiley Press, 1974.
[24] *Spatial channel model for Multiple Input Multiple Output (MIMO) simulations (Release 7), 3GPP TRZ5.996 V7.0.0*, 3GPP Standard, 2007.
[25] IST-4-027756 WINNER II: D1.1.2 V1.2 "WINNER II Channel Models," Tech. Rep., Sep. 2007.
[26] X. Dong, W. Lu, and A. C. K. Soong, "Linear interpolation in pilot symbol assisted channel estimation for OFDM," *IEEE Trans. Wireless Comm.*, vol. 6, no. 5, pp. 1910–1920, May 2007.
[27] M. T. Heath, *Scientific Computing: An Introductory Survey*, McGraw-Hill Companies, 1997.
[28] P. Tordorovic, *An Introduction to Stochastic Processes and Their Applications*, New York, Springer-Verlag, 1992.
[29] A. Abdi, J. A. Barger, and M. Kaveh, "A parametric model for the distribution of the angle of arrival and the associated correlation function and power spectrum at the mobile station," *IEEE Trans. Veh. Technol.*, vol. 61, no. 3, pp. 1222–1233, May. 2002.
[30] X. Chen, L. Li, and Y. Zhang, "A Markov model for headway/spacing distribution of road traffic," *IEEE Trans. Intell. Transp. Syst.*, vol. 11, no. 4, pp. 773–785, Dec. 2010.
[31] S. Rezaei and R. Sengupta, "Kalman filter-based integration of DGPS and vehicle sensors for localization," *IEEE Trans. Control Sys. Technol.*, vol. 15, no. 6, pp. 1080–1088, Nov. 2007.
[32] ITU-R: RS.2336-0 "Consideration of the frequency bands 1,375–1,400 MHz and 1,427–1,452 MHz for the mobile service – Compatibility with systems of the Earth exploration-satellite service (EESS) within the 1,400–1,427 MHz frequency band," Tech. Rep., 2014.
[33] A. Paier *et al.*, "First results from car-to-car and car-to-infrastructure radio channel measurements at 5.2 GHz, in *Proc. IEEE PIMRC*, 2007, pp. 1–5.
[34] J. Karedal *et al.*, "A geometry-based stochastic MIMO model for vehicle-to-vehicle communications," *IEEE Trans. Wireless Commun.*, vol. 8, no. 7, pp. 3646–3657, July 2009.
[35] P. Petrus, J. H. Reed, and T. S. Rappaport, "Geometrical-based statistical macrocell channel model for mobile environments," *IEEE Trans. Commun.*, vol. 51, no. 3, pp. 425–434, Mar. 2002.
[36] X. Cheng, C. X. Wang, D. I. Laurenson, S. Salous, and A. V. Vasilakos, "An adaptive geometry-based stochastic model for non-isotropic MIMO mobile-to-mobile channels," *IEEE Trans. Wireless Comm.*, vol. 8, no. 9 pp. 4824–4835, Sept. 2009.
[37] P. Alexander, D. Haley and A. Grant, "Cooperative intelligent transport systems: 5.9-GHz field trials," *Proc. IEEE*, vol. 99, no.7, pp. 1213–1235, July 2011.

Yan Yang was born in Sichuan, China, on Octobor 30, 1968. He received the B.Sc. degree in Electronics Engineering, and the M.Sc. and the D.Sc. degrees in Signal Processing from the University of Electronic Science and Technology of China, Sichuan University, Institute of Acoustic, Chinese Academy of Science, China, in 1990, 1997, and 2004, respectively. From 2014 to 2015, he was a visiting scholar at the Georgia Institute of Technology, Atlanta, USA. Dr. Yang is currently an Associate Professor at the State Key Lab. of Rail Traffic Control and Safety, Beijing Jiaotong University, Beijing, China. His major research interests are in wireless communications and signal processing. He received the First Research Award from the Science and Technology of China Railways Society in 2007. He is a Technical Specialist for the research item 1.11 of the Resolution 236 World Radiocommunication Conference (WRC-15), and is an active participant in the Working Party 5A (WP 5A) - Land mobile service conference excluding IMT; amateur and amateur-satellite service, the International Telecommunication Union (ITU) Radiocommunication Sector (ITU-R).

Fei Dan received his B.S., M.S. degrees in the electronics and communication engineering from Beijing Jiaotong University, Beijing, China, in 2012 and 2014, respectively. He is currently a Research Assistant with the State Key Lab. of Rail Traffic Control and Safety, Beijing Jiaotong University, Beijing, China. His research interests are wireless communications, wireless channel modeling and simulation.

Shuping Dang received the B.Eng (Hons) degree in Electrical and Electronic Engineering from the University of Manchester (with first class honors) and the B.Eng in Electrical Engineering and Automation from Beijing Jiaotong University in 2014. He was also a Certified LabVIEW Associate Developer (CLAD) by National Instrument (NI). Mr. Dang is currently a D.Phil candidate with the Department of Engineering Science, University of Oxford. His current research interests include cooperative communications and 5G communication system design.